

# Graphene: Efficient Interactive Set Reconciliation Applied to Blockchain Propagation

A. Pinar Ozisik  
Univ. of Massachusetts Amherst

Brian N. Levine  
Univ. of Massachusetts Amherst

George Bissias  
Univ. of Massachusetts Amherst

Gavin Andresen

Darren Tapp  
Dash.org

Sunny Katkuri  
Univ. of Massachusetts Amherst

## ABSTRACT

We introduce Graphene, a method and protocol for interactive set reconciliation among peers in blockchains and related distributed systems. Through the novel combination of a Bloom filter and an Invertible Bloom Lookup Table (IBLT), Graphene uses a fraction of the network bandwidth used by deployed work for one- and two-way synchronization. We show that, for this specific problem, Graphene is more efficient at reconciling  $n$  items than using a Bloom filter at the information theoretic bound. We contribute a fast and implementation-independent algorithm for parameterizing an IBLT so that it is optimally small in size and meets a desired decode rate with arbitrarily high probability. We characterize our performance improvements through analysis, detailed simulation, and deployment results for Bitcoin Cash, a prominent cryptocurrency. Our implementations of Graphene, IBLTs, and our IBLT optimization algorithm are all open-source code.

## CCS CONCEPTS

• Networks → Network protocol design.

## KEYWORDS

blockchains, set reconciliation, probabilistic data structures

### ACM Reference Format:

A. Pinar Ozisik, Brian N. Levine, George Bissias, Gavin Andresen, Darren Tapp, and Sunny Katkuri. 2019. Graphene: Efficient Interactive Set Reconciliation Applied to Blockchain Propagation. In *SIGCOMM '19: 2019 Conference of the ACM Special Interest Group on Data Communication, August 19–23, 2019, Beijing, China*. ACM, New York, NY, USA, 15 pages. <https://doi.org/10.1145/3341302.3342082>

## 1 INTRODUCTION

Minimizing the network bandwidth required for synchronization among replicas of widely propagated information is a classic need of many distributed systems. Blockchains [45, 55] and protocols for distributed consensus [17, 34] are the most recent examples of systems where the performance of network-based synchronization

is a critical factor in overall performance. Whether based on proof-of-work [33, 45], proof-of-stake [12, 27], or a directed acyclic graph (DAG) [37], the ability for these systems to scale to a large user base rely on assumptions about synchronization.

In all these systems, if the network protocol used for synchronization of newly authored *transactions* and newly mined *blocks* of validated transactions among peers is efficient, there are numerous benefits. First, if blocks can be relayed using less network data, then the maximum block size can be increased, which means an increase in the overall number of transactions per second. Scaling the transaction rate of Bitcoin is a critical performance issue [16, 18] driving many fundamental design choices such as inter-block time [55], block size, and layering [22]. Second, throughput is a bottleneck for propagating blocks larger than 20KB, and delays grow linearly with block size [16, 18]. As a consequence of the FLP result [25], blockchains cannot guarantee consensus. Smaller encodings of blocks allow for miners to reach consensus more rapidly, avoiding conflicts called *forks*. Moreover, systems based on GHOST [49], such as Ethereum [55], record forks on the chain forever, resulting in storage bloat. Finally, using less bandwidth to relay a block allows greater participation by peers who are behind limited-bandwidth links or routes (e.g., China’s firewall).

**Contributions.** In this paper, we introduce *Graphene*, a probabilistic method and protocol for synchronizing blocks (and *mempools*) with high probability among peers in blockchains and related systems. Graphene uses a fraction of the network bandwidth of related work; for example, for larger blocks, our protocol uses 12% of the bandwidth of existing deployed systems. To do so, we make novel contributions to network-based *set reconciliation* methods and the application of probabilistic data structures to network protocols. We characterize our performance through analysis, detailed simulation, and open-source deployments. Our contributions include:

- We design a new protocol that solves the problem of determining which elements in a set  $M$  stored by a receiver are members of a subset  $N \subseteq M$  chosen by a sender. We apply the solution to relaying a block of  $n = |N|$  transactions to a receiver holding  $m = |M|$  transactions. We use a novel combination of a Bloom filter [8] and an Invertible Bloom Lookup Table (IBLT) [30]. Our approach is smaller than using current deployed solutions [15] and previous IBLT-based approximate solutions [23]. We show our solution to this specific problem is an improvement of  $\Omega(n \log n)$  over using an optimal Bloom filter alone.
- We extend our solution to the more general case where some of the elements of  $N$  are not stored by the receiver. Thus, our protocol extension handles the case where a receiver is missing transactions in the sender’s block; our solution is a small fraction

Permission to make digital or hard copies of all or part of this work for personal or classroom use is granted without fee provided that copies are not made or distributed for profit or commercial advantage and that copies bear this notice and the full citation on the first page. Copyrights for components of this work owned by others than ACM must be honored. Abstracting with credit is permitted. To copy otherwise, or republish, to post on servers or to redistribute to lists, requires prior specific permission and/or a fee. Request permissions from [permissions@acm.org](mailto:permissions@acm.org).

*SIGCOMM '19, August 19–23, 2019, Beijing, China*

© 2019 Association for Computing Machinery.

ACM ISBN 978-1-4503-5956-6/19/08...\$15.00

<https://doi.org/10.1145/3341302.3342082>

of the size of previous work [54] at the cost of an additional message. Additionally, we show how Graphene can efficiently identify transactions held by the receiver but not the sender.

- We design and evaluate an efficient search algorithm for parameterizing an IBLT so that it is optimally small in size but meets a desired decode rate with arbitrarily high probability. Because it is based on a hypergraph representation, it has faster execution times. This result is applicable beyond our context to any use of IBLTs.
- We design and evaluate a method for significantly improving the decode rate of an IBLT when two IBLTs are available that are based on roughly the same set of elements. This method is also generally applicable.
- We provide a detailed evaluation using theoretical analysis and simulation to quantify performance against existing systems. We also characterize performance of our protocol in a live Bitcoin Cash deployment, and in an Ethereum implementation for historic blocks. We also show that Graphene is more resilient to attack than previous approaches.

We have publicly released our Bitcoin Cash and Ethereum implementations of Graphene [3, 31], a C++ and Python implementation of IBLTs including code for finding their optimal parameters [36], and we have released a public network specification of our basic protocol for standard interoperability [5]. It has been adopted by blockchain developers in released clients, replacing past approaches [6, 7]. While our focus is on blockchains, our work applies in general to systems that require set reconciliation, such as database or file system synchronization among replicas. Or for example systems such as CRLite [35], where a client regularly checks a server for revocations of observed certificates.

This submission extends and improves upon the authors' previous workshop paper [46]. The contributions of our prior work included only the first bullet above (i.e., Protocol 1 in Section 3.1) and empirical simulations of its performance. All other contributions listed above are new. This work does not raise any ethical issues.

## 2 BACKGROUND AND RELATED WORK

Below, we summarize and contrast related work in network-based set reconciliation and protocols for block propagation.

### 2.1 Set Reconciliation Data Structures

*Set reconciliation* protocols allow two peers, each holding a set, to obtain and transmit the union of the two sets. This synchronization goal is distinct from set membership protocols [14], which tell us, more simply, if an element is a member of a set. However, data structures that test set membership are useful for set reconciliation. This includes Bloom filters [8], a seminal probabilistic data structure with myriad applications [10, 39, 51]. Bloom filters encode membership for a set of size  $n$  by inserting the items into a small array of  $\frac{-n \log_2(f)}{\ln(2)}$  bits. Each item is inserted  $k = \log(2)m/n$  times using independent hash functions. This efficiency gain comes at the expense of allowing a false positive rate (FPR),  $f$ .

Invertible Bloom Lookup Tables (IBLTs) [30] are a richer probabilistic data structure designed to recover the *symmetric difference* of two sets of items. Like Bloom filters, items are inserted into an

IBLT's array of  $c$  cells, which is partitioned into subsets of size  $c/k$ . Each item is inserted once into each of the  $k$  partitions, at indices selected by  $k$  hash functions. Rather than storing only a bit, the cells store aggregates of the actual items. Each cell has a *count* of the number of items inserted and the xor of all items inserted (called a *keySum*). The following algorithm [23] recovers the symmetric difference of two sets. Each set is stored in an IBLT,  $A$  and  $B$ , respectively, (with equal  $c$  and  $k$  values). For each pairwise cell of  $A$  and  $B$ , the keySums are xored and the counts subtracted, resulting in a third IBLT:  $A \Delta B = C$  that lacks items in the intersection. The cells in  $C$  with count = 1 hold an item belonging to only  $A$ , and to only  $B$  if count = -1. These items are removed from the  $k - 1$  other cells, which decrements their counts and allows for the additional *peeling* of new items. This process continues until all cells have a count of 0. (A *checkSum* field catches a special case: if  $x$  values in a cell from  $A$  and  $x - 1$  values that are not a subset from the corresponding cell in  $B$  are subtracted, then count = 1 but the value contained is part of neither set.) If  $c$  is too small given the actual symmetric difference, then iterative peeling will eventually fail, resulting in a *decode failure*, and only part of the symmetric difference will be recovered.

There are many variations of Bloom filters that present different trade-offs, such as more computation for smaller size. Similarly, IBLTs are one of several alternatives. For example, several approaches involve more computation but are smaller in size [21, 41, 56] (see [23] for a comparison). We have not investigated how alternatives to IBLTs improve Graphene's size nor how, for example, computational costs differ. Our focus is on IBLTs because they are balanced: minimal computational costs and small size. While miners may have strong computational resources, *full nodes* and lighter clients in blockchains may not. More importantly, as our deployment results in Section 5.3 show, Graphene's size grows slowly as block size increases for the most likely scenarios in Bitcoin, Bitcoin Cash, and Ethereum, demonstrating that IBLTs are a good fit for our problem. Finally, some of these solutions are complementary; for example, *minsketch* [56] can be used within the cells of IBLTs to reduce Graphene's size further.

**Comparison to related work.** We provide a novel solution to the problem of set reconciliation, where one-way or mutual synchronization of information is required by two peers. Our results are significantly better than deployed past work that is based on Bloom filters alone [54] or IBLTs alone [23, 30], as we show in Section 5.3.

Byers et al. [13] introduce a new data structure called Approximate Reconciliation Trees (ARTs), based on Merkle trees, for set reconciliation. Their focus is different than ours, as their goal is not to discover the exact symmetric difference between two sets held by sender and receiver. Eppstein et al. [23] also present a set reconciliation solution, based primarily on IBLTs. They show their approach is more efficient for symmetric differences of 10k or fewer than ARTs as well as Characteristic Polynomial Interpolation [41], which is another solution to set reconciliation. Our method is more efficient than these past approaches for discovering the exact symmetric difference in terms of storage or computation or both.

We provide several contributions to IBLTs. In general, if one desires to decode sets of size  $j$  from an IBLT, a set of values  $\tau > 0$  and  $k > 2$  must be found that result in  $c = j\tau$  cells (divisible by  $k$ )

such that the probability of decoding is at least  $p$ . We provide an implementation-independent algorithm for finding values  $\tau$  and  $k$  that meet rate  $p$  and result in the smallest value of  $c$ .

Our work advances the usability of IBLTs. Goodrich and Mitzenmacher [30] provide values of  $\tau$  that *asymptotically* ensure a failure rate that decreases polynomially with  $j$ . But these asymptotic results are not optimally small in size for finite  $j$  and do not help us set the value of  $k$  optimally. Using their unreleased implementation, Eppstein et al. [23] identify optimal  $\tau$  and  $k$  that meet a desired decode rate for a selection of  $j$  values; however, the statistical certainty of this optimality is unclear. In comparison, using our open-source IBLT implementation [36], we are able to systematically produce statistically optimal values for  $\tau$  and  $k$  (within a finite search range) for a wide range of  $j$  values. Because our method is based on hypergraphs, it is an order of magnitude faster than this previous method [23].

We also contribute a novel method for improving the decode rate of IBLTs that is similar in approach to Gollakota and Kitabi [28]. Our method is complementary to related work by Pontarelli et al. [47], who have the same goal.

## 2.2 Block Propagation

Blockchains, distributed ledgers, and related technologies require a network protocol for distributing new transactions and new blocks. Almost all make use of a p2p network, often a clique among *miners* that validate blocks, and a random topology among non-mining *full* nodes that store the entire chain. New transactions have an ID equal to their cryptographic hash. When a new transaction is received, a peer sends the ID as the contents of an inventory (*inv*) message to all  $d$  neighbors, who request a *getdata* message if the transaction is new to them. Transactions are stored in a *mempool* until included in a valid block. Blocks are relayed similarly: an *inv* is sent to each neighbor (often the header is sent instead to save time), and a *getdata* requests the block if needed. The root of a Merkle tree [40] of all transactions validates an ordered set against the mined block.

The block consists of a header and a set of transactions. These transactions can be relayed by the sender in *full*, but this wastes bandwidth because they are probably already stored by the receiver. In other words, blocks can be relayed with a compressed encoding, and a number of schemes have been proposed. As stated in Section 1, efficient propagation of blocks is critical to achieving consensus, reducing storage bloat, overcoming network firewall bottlenecks, and allowing scaling to a large number of transactions per second.

Transactions that offer low fees to miners are sometimes marked as DoS spam and not propagated by full nodes; yet, they are sometimes included in blocks, regardless. To avoid sending redundant *inv* messages, peers keep track, on a per-transaction and per-neighbor basis, whether an *inv* has been exchanged. This log can be used by protocols to send missing transactions to a receiver proactively as the block is relayed.

**Comparison to related work.** *Xtreme Thinblocks* [54] (XThin) is a robust and efficient protocol for relaying blocks, and is deployed in Bitcoin Unlimited (BU) clients. The receiver’s *getdata* message includes a Bloom filter encoding the transaction IDs in her mempool. The sender responds with a list of the block’s transaction IDs

shortened to 8-bytes (since the risk of collision is still low), and uses the Bloom filter to also send any transactions that the receiver is missing. XThin’s bandwidth increases with the size of the receiver’s mempool, which is likely a multiple of the block size. In comparison, Graphene uses significantly lower bandwidth both when the receiver is and is not missing transactions. However, Graphene may use an additional roundtrip time to repair missing transactions.

*Compact Blocks* [15] is a protocol that is deployed in the Bitcoin Core, Bitcoin ABC, and Bitcoin Unlimited clients. In this protocol, the receiver’s *getdata* message is a simple request (no Bloom filter is sent). The sender replies with the block’s transaction IDs shorted to 6-bytes (as well as the coinbase transaction). If the receiver has missing transactions, she requests repairs with a followup *inv* message. Hence, the network cost is  $6n$  bytes, which is smaller than XThin’s cost of a Bloom filter and a list of transaction IDs, which is approximately  $\frac{m \log_2(f)}{8 \ln(2)} + 6n$ ; however, when the receiver is missing transactions, Compact Blocks has an extra roundtrip time, which may cost more if enough transactions are missing. Graphene is significantly lower in cost than Compact Blocks, as we show in Section 5.3.

Recently, *Xthinner* [52] was proposed as a variant of Xthin that employs compression techniques on the list of transactions in a block. Since the author states that Xthinner is not as compact as Graphene, we do not compare against it [53].

## 3 THE GRAPHENE PROTOCOL

The primary goal of Graphene is to reduce the amount of network traffic resulting from synchronization of a sender and receiver; we do so in the context of block propagation. To motivate Graphene, consider a protocol that uses a Bloom filter alone to encode a block containing  $n$  transactions. Assume the receiver has a mempool of  $m$  transactions that are a super set of the sender’s block. If we set the FPR of the sender’s Bloom filter to  $f = \frac{1}{144(m-n)}$ , then we can expect the filter to falsely include an extra transaction in a relayed block about once every 144 blocks (approximately once a day in Bitcoin). This approach requires  $\frac{-n \log_2(f)}{8 \ln(2)}$  bytes, and it is easy to show that it is smaller than Compact Blocks ( $6n$  bytes) when  $m < 71,982,340 + n$ , which is highly likely.

But we can do better than using a Bloom filter alone: in Graphene, we shrink the size of the sender’s Bloom filter by increasing its FPR, and we correct any false positives at the receiver with an IBLT. The summed size of the two structures is smaller than using either alone. In practice, our technique performs significantly better than Compact Blocks for all but the smallest number of transactions, and we show in Section 5.3 that it performs better than *any* Bloom-filter-only approach asymptotically.

We design two protocols for Graphene, which we define presently. Both protocols use probabilistic data structures that fail with a tunable probability. Throughout our exposition, we use the concept of probabilistic *assurance*. Specifically, a property  $A$  is said to be held in data structure  $X$  with  $\beta$ -assurance whenever it is possible to tune  $X$  so that  $A$  occurs in  $X$  with probability at least  $\beta$ .

In **Protocol 1**, we assume that the receiver’s mempool contains all transactions in the block, a typical case due to the aggressive synchronization that blockchains employ. So, our first design choice

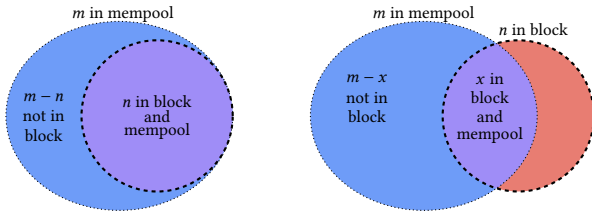


**Figure 1: (Left) The receiver’s mempool contains the entire block; Protocol 1: Graphene manages this scenario. (Right) The receiver’s mempool does not contain the entire block. Protocol 2: Graphene Extended manages this scenario.**

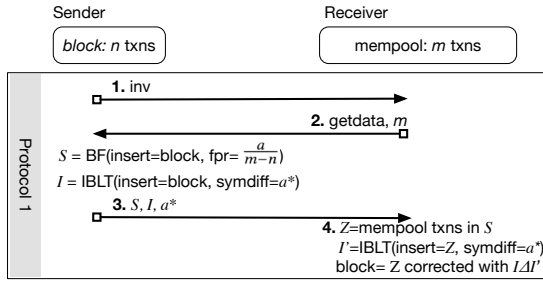


**Figure 2: An illustration of Protocol 1 for propagating a block that is a subset of the mempool.**

is to optimize for this scenario illustrated in Fig. 1-Left. As we show in Section 5.3, Protocol 1 is usually enough to propagate blocks.

In **Protocol 2**, we do not assume that the receiver’s mempool is synchronized, as illustrated in Fig. 1-Right, which allows us to apply it to two scenarios: (i) block relaying between unsynchronized peers; and (ii) intermittent mempool synchronization. A receiver may not be synchronized with the sender because of network failures, slow transaction propagation times relative to blocks, or if the block contains unpropagated low-fee transactions erroneously filtered out as spam. Protocol 2 begins when Protocol 1 fails: the receiver requests missing transactions using a second Bloom filter; and the sender transmits any missing transactions, along with a second IBLT to correct mistakes. (Compact Blocks and XThin also handle this scenario but do so with greater network bandwidth.)

### 3.1 Protocols

Our first protocol is for receivers whose mempool contains all the transactions in the block; see Fig. 1-Left. The protocol is illustrated in Fig. 2.

#### PROTOCOL 1: Graphene

- 1: Sender: The sender transmits an *inv* (or blockheader) for a block.
- 2: Receiver: The receiver requests the unknown block, including a count of transactions in her mempool, *m*.
- 3: Sender: The sender creates Bloom filter **S** and IBLT **I** from the transaction IDs of the block (purple area in Fig. 1-Left). The FPR of **S** is  $f_S = \frac{a}{m-n}$ , and the IBLT is parameterized such that  $a^*$  items can be recovered, where  $a^* > a$  with  $\beta$ -assurance

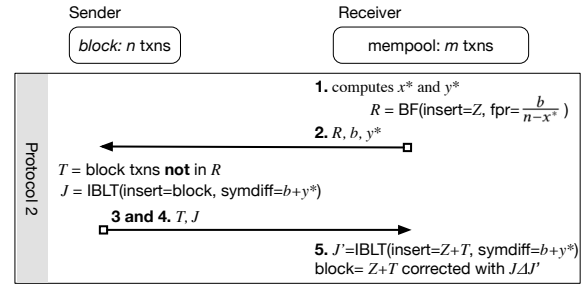


**Figure 3: If Protocol 1 fails (e.g., if the block is not a subset of the mempool), Protocol 2 recovers with one roundtrip.**

(outlined in green in Fig. 4). We set *a* so as to minimize the total size of **S** and **I**. **S** and **I** are sent to the receiver along with the block header (if not sent in Step 1).

- 4: Receiver: The receiver creates a candidate set *Z* of transaction IDs that pass through **S**, including false positives (purple and dark blue areas in Fig. 4). The receiver also creates IBLT **I'** from *Z*. She *subtracts*  $\mathbf{I} \Delta \mathbf{I}'$ , which evaluates to the symmetric difference of the two sets [23]. Based on the result, she adjusts the candidate set, validates the Merkle root in the block header, and decodes the block.

In blockchains, the sender knows the transactions for which no *inv* message has been exchanged with the receiver<sup>1</sup>; those transactions could be sent at Step 3 in order to reduce the number of transactions in  $\mathbf{I} \Delta \mathbf{I}'$ . (N.b., the IBLT stores only 8 bytes of each transaction ID; but full IDs are used for the Bloom filter.)

We use a fast algorithm to select *a* such that the total amount of data transmitted over the network is optimally small; see Section 3.3.1. The count of false positives from **S** has an expected mean of  $(m - n)f_S = a$ , whose variance comes from a Binomial distribution with parameters  $(m - n)$  and  $f_S$ . Because of this variance,  $a^*$  should be used to parameterize **I** instead of *a*. We derive  $a^*$  in Section 3.3.1 via a Chernoff bound.

### 3.2 Graphene Extended

If the receiver does not have all the transactions in the block (Fig. 1-Right), IBLT subtraction in Protocol 1 will not succeed. In that case, the receiver should continue with the following protocol, illustrated in Fig. 3. Subsequently, we show how this protocol can also be used for intermittent mempool synchronization. Our contribution is not only the design of this efficient protocol, but the derivation of parameters that meet a desired decode rate.

#### PROTOCOL 2: Graphene Extended

- 1: Receiver: The size of the candidate set is  $|Z| = z$ , where  $z = x + y$ , a sum of *x* true positives and *y* false positives (purple and dark blue areas in Fig. 5). Because the values of *x* and *y* are obfuscated within the sum, the receiver calculates  $x^*$  such that  $x^* \leq x$  with  $\beta$ -assurance (green outline in Fig. 5) She also

<sup>1</sup>In theory peers know this information; but in practice they use lossy data structures to keep track of this information.

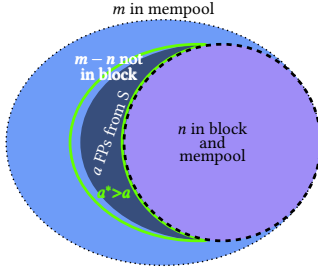


Figure 4: [Protocol 1] Passing  $m$  mempool transactions through  $S$  results in  $a$  FPs (in dark blue). A green outline illustrates  $a^* > a$  with  $\beta$ -assurance, ensuring IBLT  $I$  decodes.

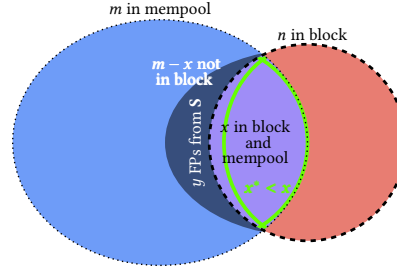


Figure 5: [Protocol 2] Passing  $m$  transactions through  $S$  results in  $z$  positives, obscuring a count of  $x$  TPs (purple) and  $y$  FPs (in dark blue). From  $z$ , we derive  $x^* < x$  with  $\beta$ -assurance (in green).

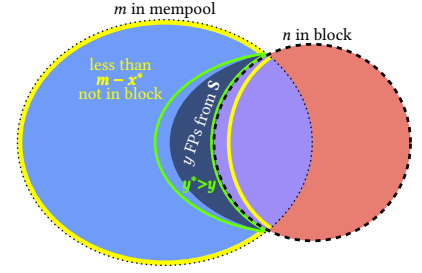


Figure 6: [Protocol 2] From our bound  $m - x^* > m - x$  with  $\beta$ -assurance (in yellow), we can derive a bound for the false positives from  $S$  as  $y^* > y$  with  $\beta$ -assurance outlined in green.

calculates  $y^*$  such that  $y^* \geq y$  with  $\beta$ -assurance (green outline in Fig. 6).

- 2: Receiver: The receiver creates Bloom filter  $\mathbf{R}$  and adds all transaction IDs in  $Z$  to  $\mathbf{R}$ . The FPR of the filter is  $f_R = \frac{b}{n-x^*}$ , where  $b$  minimizes the size of  $\mathbf{R}$  and IBLT  $\mathbf{J}$  in step 4. She sends  $\mathbf{R}$ ,  $y^*$  and  $b$ .
- 3: Sender: The sender passes all transaction IDs in the block through  $\mathbf{R}$ . She sends all transactions that are not in  $\mathbf{R}$  directly to the receiver (red area of Fig. 6)
- 4: Sender: The sender creates and sends an IBLT  $\mathbf{J}$  of all transactions in the block such that  $b + y^*$  items can be recovered from it. This size accounts for  $b$ , the number of transactions that falsely appear to be in  $\mathbf{R}$ , and  $y^*$ , the number of transactions that falsely appear to be in  $\mathbf{S}$ .
- 5: Receiver: The receiver creates IBLT  $\mathbf{J}'$  from the transaction IDs in  $Z$  and the new transaction IDs sent by the sender in step 3. She decodes the subtraction of the two blocks,  $\mathbf{J} \Delta \mathbf{J}'$ . From the result, she adjusts set  $Z$ , validates the Merkle root, and decodes the block.

As in Protocol 1, we set  $b$  so that the summed size of  $\mathbf{R}$  and  $\mathbf{J}$  is optimally small; see Section 3.3.1. We also derive solutions for  $x^*$  and  $y^*$ ; see Section 3.3.2.

### 3.2.1 Mempool Synchronization.

With a few changes, Protocols 1 and 2 can be used by two peers to synchronize their mempools so that both parties obtain the union of the two mempools, instead of a block that is a subset of one of the mempools. In this context, instead of a block, the sender places his entire mempool in  $\mathbf{S}$  and  $\mathbf{I}$ . The receiver passes her mempool through  $\mathbf{S}$ , adding any negatives to  $H$ , the set of transactions that are not in  $\mathbf{S}$ . Some transactions that the sender does not have in his mempool will falsely pass through  $\mathbf{S}$ , and these are identified by  $\mathbf{I}$  (assuming that it decodes); these transactions are also added to  $H$ . If  $\mathbf{I}$  does not decode, Protocol 2 is executed to find transactions in the symmetric difference of the mempools; all missing transactions among the sender and receiver are exchanged, including those in set  $H$ . The protocol is more efficient if the peer with the smaller mempool acts as the sender since  $\mathbf{S}$  will be smaller. Section 5.3.2 shows that the protocol is efficient.

## 3.3 Ensuring Probabilistic Data Structure Success

Cryptocurrencies allow no room for error: the header's Merkle root can be validated with an exact set of transactions only. Yet, Graphene is a probabilistic solution, and if its failure rate is high, resources are wasted on recovery. In this section, we derive the parameters for Graphene that ensure a tunable, high success rate.

### 3.3.1 Parameterizing Bloom filter $\mathbf{S}$ and IBLT $\mathbf{I}$ .

Graphene sends the least amount of data over the network when the sum of the Bloom filter  $\mathbf{S}$  and IBLT  $\mathbf{I}$  is minimal. Let  $T = T_{BF} + T_I$  be the summed size of the Bloom filter and IBLT. The size of a Bloom filter in bytes,  $T_{BF}$ , with false positive rate  $f_S$  and  $n$  items inserted is  $T_{BF} = \frac{-n \ln(f_S)}{8 \ln^2 2}$  [8]. Recall that we recover up to  $a^*$  items from the IBLT, where  $a^* > a$  with  $\beta$ -assurance. As we show in Section 3.3.1,  $a^* = (1 + \delta)a$ , where  $\delta$  is parameterized by  $\beta$ . An IBLT's size is a product of the number of items recoverable from a symmetric difference and a multiplier  $\tau$  that ensures recovery at a desired success rate. Therefore, given the cost of  $r$  bytes per cell,  $T_I$  is

$$T_I = r\tau(1 + \delta)a. \quad (1)$$

When we set  $f_S = \frac{a}{m-n}$ , the total size of the Bloom filter and IBLT in bytes is

$$T(a) = \frac{-n \ln(\frac{a}{m-n})}{8 \ln^2 2} + r\tau(1 + \delta)a. \quad (2)$$

The value of  $a$  that minimizes  $T$  is either:  $a = 1$ ;  $a = m - n$ ; or the value of  $a$  where the derivative of Eq. 2 with respect to  $a$  is equal to zero. When  $\delta = 0$  this is equal to

$$a = n/(8r\tau \ln^2 2). \quad (3)$$

Eq. 3 is a good approximation for the minimum when  $\delta$  is close to 0; and the exact value is difficult to derive. Furthermore, implementations of Bloom filters and IBLTs involve non-continuous ceiling functions. As a result, Eq. 3 is accurate only for  $a \geq 100$ ; otherwise the critical point  $a'$  produced by Eq. 3 can be inaccurate enough that  $T(a')$  is as much as 20% higher than its true minimum value. Graphene exceeds the performance of previous work when Eq. 3 is used to select  $a$ . However, implementations that desire strictly optimal performance should take an extra step. If Eq. 3 results in a value of  $a$  less than 100, its size should be computed using accurate

ceiling functions and compared against all points  $a < 100$ . This is a typical case in our implementation for current block sizes.

**Derivation of  $a^*$ .** We can parameterize IBLT **I** based on the expected number of false positives from **S**, but to ensure a high decode rate, we must account for the natural variance of false positives generated by **S**. Here we derive a closed-form expression for  $a^*$  as a function of  $a$  and  $\beta$  such that  $a^* > a$  holds with  $\beta$ -assurance, i.e.  $a^* > a$  with probability at least  $\beta$ . Define  $A_1, \dots, A_{m-n}$  to be independent Bernoulli trials such that  $\Pr[A_i = 1] = f_S$ ,  $A = \sum_{i=1}^{m-n} A_i$ , and  $\mu = E[A]$ .

**THEOREM 1:** *Let  $m$  be the size of a mempool that contains all  $n$  transactions from a block. If  $a$  is the number of false positives that result from passing the mempool through Bloom filter **S** with FPR  $f_S$ , then  $a^* \geq a$  with probability  $\beta$  when*

$$a^* = (1 + \delta)a,$$

$$\text{where } \delta = \frac{1}{2}(s + \sqrt{s^2 + 8s}) \text{ and } s = \frac{-\ln(1-\beta)}{a}.$$

A full proof appears in Appendix A. According to Theorem 1, if the sender sends a Bloom filter with FPR  $f_S = \frac{a}{m-n}$ , then with  $\beta$ -assurance, no more than  $a^*$  false positives will be generated by passing elements from **Z** through **S**. To compensate for the variance in false positives, IBLT **I** is parameterized by a symmetric difference of  $a^* = (1 + \delta)a$  items. **I** will decode subject to its own error rate (see Section 4), provided that  $a < a^*$  (which occurs with probability  $\beta$ ) and the receiver has all  $n$  transactions in the block. We evaluate this approach in Section 5.3; see Fig. 15.

### 3.3.2 Parameterizing Bloom filter **R** and IBLT **J**.

**Parameterizing  $b$ .** In Protocol 2, we select  $b$  so that the summed size of **R** and **J** is optimally small. Its derivation is similar to  $a$ . We show below that  $y^* = (1 + \delta)y$ . Thus, for protocol 2 the total size is:

$$T(b) = \frac{z \ln(\frac{b}{n-x^*})}{8 \ln^2 2} + r\tau(1 + \delta)b. \quad (4)$$

When  $\delta = 0$ , the optimal value of  $b$  assuming continuous values is

$$b = z/(8r\tau \ln^2 2). \quad (5)$$

Similar to Section 3.3.1, an exact closed form for  $b$  is difficult to derive; and a perfectly optimal implementation would compute  $T(b)$  using ceiling functions for values of  $b < 100$ .

**Using  $z$  to parameterize **R** and **J**.** Here we offer a closed-form solution to the problem of parameterizing Bloom filter **R** and IBLT **J**. This is a more challenging problem because  $x$  and  $y$  cannot be observed directly.

Let  $z$  be the observed count of transactions that pass through Bloom filter **S**. We know that  $z = x + y$ : the sum of  $x$  true positives and  $y$  false positives, illustrated as **purple** and **dark blue** areas respectively in Fig. 5. Even though  $x$  is unobservable, we can calculate a lower bound  $x^*$ , depending on  $x, z, m, f_S$  and  $\beta$ , such that  $x^* \leq x$  with  $\beta$ -assurance, illustrated as a **green** outline in Fig. 5.

With  $x^*$  in hand, we also have, with  $\beta$ -assurance, an upper bound on the number of transactions the receiver is missing:  $n - x^* > n - x$ . This bound allows us to conservatively set  $f_R = \frac{b}{n-x^*}$  for Bloom

filter **R**. In other words, since  $x^* < x$  with  $\beta$ -assurance, the sender, using **R**, will fail to send no more than  $b$  of the  $n - x$  transactions actually missing at the receiver. IBLT **J** repairs these  $b$  failures, subject to its own error rate (see Section 4).

We also use  $x^*$  to calculate, with  $\beta$ -assurance, an upper bound  $y^* \geq y$  on the number of false positives that pass through **S**. The **green** area in Fig. 6 shows  $y^*$ , which is a superset of the actual value for  $y$ , the **dark blue** area.

The sender's IBLT **J** contains all transactions in the block. The receiver's IBLT **J'** contains true positives from **S**, false positives from **S**, and newly sent transactions. Therefore, we bound both components of the symmetric difference by  $b + y^*$  transactions in order for the subtraction operation to decode. In other words, both **J** and **J'** are parameterized to account for more items than actually exist in the symmetric difference between the two IBLTs. Note that we use  $\beta$ -assurance to bound the performance of each probabilistic data structure; in doing so, we establish worst-case performance guarantees for our protocol.

The following theorems derive values for  $x^*$  and  $y^*$ .

**THEOREM 2:** *Let  $m$  be the size of a mempool containing  $0 \leq x \leq n$  transactions from a block. Let  $z = x + y$  be the count of mempool transactions that pass through **S** with FPR  $f_S$ , with true positive count  $x$  and false positive count  $y$ . Then  $x^* \leq x$  with probability  $\beta$  when*

$$x^* = \arg \min_{x^*} \Pr[x \leq x^*; z, m, f_S] \leq 1 - \beta.$$

$$\text{where } \Pr[x \leq k; z, m, f_S] \leq \sum_{i=0}^k \left( \frac{e^{\delta_k}}{(1 + \delta_k)^{1 + \delta_k}} \right)^{(m-k)f_S}$$

$$\text{and } \delta_k = \frac{z - k}{(m - k)f_S} - 1.$$

A full proof appears in Appendix A.

**THEOREM 3:** *Let  $m$  be the size of a mempool containing  $0 \leq x \leq n$  transactions from a block. Let  $z = x + y$  be the count of mempool transactions that pass through **S** with FPR  $f_S$ , with true positive count  $x$  and false positive count  $y$ . Then  $y^* \geq y$  with probability  $\beta$  when*

$$y^* = (1 + \delta)(m - x^*)f_S,$$

$$\text{where } \delta = \frac{1}{2}(s + \sqrt{s^2 + 8s}) \text{ and } s = \frac{-\ln(1-\beta)}{(m-x^*)f_S}.$$

A full proof appears in Appendix A.

**Special case:  $m \approx n$ .** When  $m \approx n$ , our optimization procedure in Protocol 1 will parameterize  $f_S$  to a value near 1, which is very efficient if the receiver has all of the block. But if  $m \approx n$  and the receiver is missing some portion of the block, Protocol 1 will fail. Subsequently, with  $z \approx m$ , Protocol 2 will set  $y^* \approx m$  and  $x^* \approx 0$ , and  $f_R \approx 1$ ; and most importantly, IBLT **J** will be sized to  $m$ , making it larger than a regular block.

Fortunately, resolution is straightforward. If Protocol 1 fails, and the receiver finds that  $z \approx m$ ,  $y^* \approx m$ , and  $f_R \approx 1$ , then in Step 2 of Protocol 2, the receiver should set  $f_R$  to a value less than 1. We set

$f_R = 0.1$ , but a large range of values execute efficiently (we tested from 0.001 to 0.2). All mempool transactions that pass through **S** are inserted into Bloom filter **R**, and **R** is transmitted to the sender.

The sender follows the protocol as usual, sending IBLT **J** along with  $h$  transactions from the mempool not in **R**. However, he then deviates from the protocol by also sending a third Bloom filter **F** intended to compensate for false positives from **R**. The  $n - h$  transactions that pass through **R** are inserted into **F**. The roles of Protocol 2 are thus reversed: the sender uses Theorems 2 and 3 to solve for  $x^*$  and  $y^*$ , respectively, to bound false positives from **R** (substituting the block size for mempool size and  $f_R$  as the FPR). He then solves for  $b$  such that the total size in bytes is minimized for **F** with FPR  $f_F = \frac{b}{m-x^*}$  and **J** having size  $b + y^*$ . This case may be common when Graphene is used for mempool synchronization; our evaluations in Fig. 18 in Section 5.3.2 show that this method is more efficient than Compact Blocks.

**Alternatives to Bloom filters.** There are dozens of variations of Bloom filters [39, 51], including Cuckoo Filters [24] and Golomb Code sets [29]. Any alternative can be used if Eqs. 2, 3, 4, and 5 are updated appropriately.

#### 4 ENHANCING IBLT PERFORMANCE

The success and performance of Graphene rests heavily on IBLT performance. Using IBLTs over a network has been studied in only a handful of papers [9, 23, 30, 42, 47], and current results are generally asymptotic with the size of the IBLT (the notable exception is Eppstein et al. [23], which we discuss in Section 2). In this section, we contribute several important results that allow for IBLTs to be used in practical systems with reliable precision. IBLTs are deceptively challenging to parameterize so that  $j$  items can be recovered with a desired success probability of  $p$ , using the minimal number of cells. Only two parameters can be set: the *hedge* factor,  $\tau$  (resulting in  $c = j\tau$  cells total), and the number of hash functions,  $k$ , used to determine where to insert an item (each function covers  $c/k$  cells).

**Motivation.** Fig. 7 motivates our contributions, showing the poor decode rate of an IBLT if static values for  $k$  and  $\tau$  are applied to small values of  $j$ . The figure shows three desired decode failure rates ( $1-p$ ) in magenta: 1/24, 1/240, and 1/2400. The black points show the decode failure probability we observed in our IBLT implementation for static settings of  $\tau = 1.5$  and  $k = 4$ . The resulting decode rate is either too small from an under-allocated IBLT, or exceeds the rate through over-allocation. The colored points show the failure rates of actual IBLTs parameterized by the algorithm we define below: they are optimally small and always meet or exceed the desired decode rate.

##### 4.1 Optimal Size and Desired Decode Rate

Past work has never defined an algorithm for determining size-optimal IBLT parameters. We define an implementation-independent algorithm, adopting Malloy’s [44] and Goodrich et al.’s interpretation [30] of IBLTs as uniform hypergraphs.

Let  $H = (V, X, k)$  be a  $k$ -partite,  $k$ -uniform hypergraph, composed of a set of  $c$  vertices. Let  $V = V_1 \cup \dots \cup V_k$ , where each  $V_i$  is a subset of  $c/k$  vertices (we enforce that  $c$  is divisible by  $k$ ).  $X$  is a set of  $j$  hyper-edges, each connecting  $k$  vertices, one from each of the  $V_i$ .

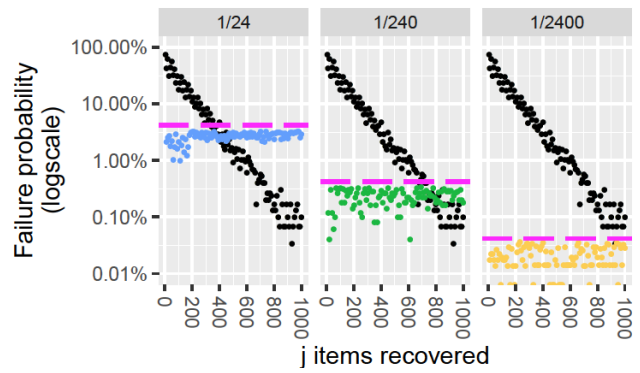


**Figure 7: Parameterizing an IBLT statically results in poor decode rates. The black points show the decode failure rate for IBLTs when  $k = 4$  and  $\tau = 1.5$ . The blue, green and yellow points show decode failure rates of optimal IBLTs, which always meet a desired failure rate on each facet (in magenta). Size shown in Fig. 10.**

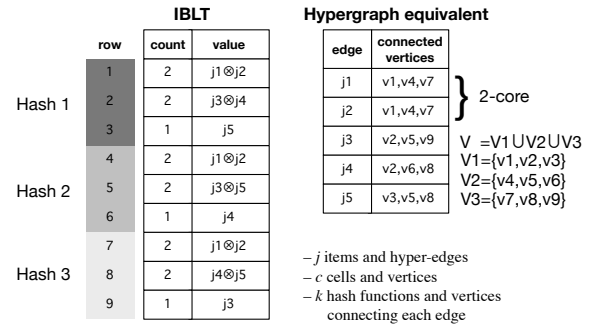


**Figure 8: An example IBLT (without the checksum field) and its equivalent hypergraph representation. In the IBLT,  $k = 3$ , there are  $c = 3k$  cells, and  $j = 5$  items are placed in  $k$  cells. In the hypergraph,  $j$  hyperedges each have  $k$  vertices out of  $c$  vertices total.**

The hypergraph represents an IBLT with  $k$  hash functions,  $j$  inserted items, and  $c$  cells. As illustrated in Figure 8, each cell corresponds to a vertex, and we have  $|V| = c$  and  $|V_i| = c/k$ . Each item represents an edge connecting  $k$  vertices, with the  $i$ th vertex being chosen uniformly at random from  $V_i$ . Vertices in  $V_i$  correspond to hash function  $i$ , which operates over a distinct range of cells.

Decoding corresponds to removing edges that contain a vertex of degree 1, repeatedly. The  $r$ -core [48] of  $H$  is the maximal subgraph (after decoding) in which all vertices have degree at least  $r$ .  $H$  contains a non-empty 2-core iff the IBLT it represents cannot be decoded. In the example illustrated in Figure 8, edges  $j_3, j_4$  and  $j_5$  contain degree 1 vertices  $v_9, v_6$ , and  $v_3$  respectively and can be removed; the remaining subgraph comprised of  $j_1$  and  $j_2$  and degree 2 vertices  $v_1, v_4$ , and  $v_7$  is a 2-core. Equivalent operations on the IBLT would show that items  $j_1$  and  $j_2$  cannot be decoded.

We seek an algorithm for determining the most space-efficient choice for  $c$  and  $k$  that is sufficient to ensure a decode rate of  $p$  for a fixed number of inserted items  $j$ . Items are inserted pseudo-randomly by applying the hash functions. Therefore, it makes sense to model the edge set  $X$  as a random variable. Define  $\mathcal{H}_{j,p} =$

**ALGORITHM 1: IBLT-Param-Search**

```

01 SEARCH( $j, k, p$ ):
02  $c_l = 1$ 
03  $c_h = c_{max}$ 
04  $trials = 0$ 
05  $success = 0$ 
06  $L = (1 - p)/5$ 
07 WHILE  $c_l \neq c_h$ :
08    $trials += 1$ 
09    $c = (c_l + c_h)/2$ 
10   IF decode( $j, k, c$ ):
11      $success += 1$ 
12    $conf = conf\_int(success, trials)$ 
13    $r = success/trials$ 
14   IF  $r - conf \geq p$ :
15      $c_h = c$ 
16   IF  $(r + conf \leq p)$ :
17      $c_l = c$ 
18   IF  $(r - conf > p - L)$  and  $(r + conf < p + L)$ :
19      $c_l = c$ 
20 RETURN  $c_h$ 

```

**Figure 9:** This algorithm searches for the optimally small size of  $c = j\tau$  cells that decodes  $j$  items with decode success probability  $p$  (within appropriate confidence intervals) from an IBLT with  $k$  hash functions. `decode()` operates over a hypergraph rather than a real IBLT.

$\{(V, X, k) \mid E[\text{decode}((V, X, k))] \geq p, |X| = j\}$ , or the set of hypergraphs  $(V, X, k)$  on  $j$  edges whose expected decode success rate is bounded by  $p$ . Based on this definition, the algorithm should return

$$\arg \min_{(V, X, k) \in \mathcal{H}_{j,p}} |V|. \quad (6)$$

Our approach for solving Eq. 6 is to fix  $j, p$ , and  $k$  and perform binary search over all possible values for  $c = |V|$ . A key point is that binary search is justified by the fact that the expected decode failure rate is a monotonically increasing function of  $c$ . This notion can be explained as follows. A 2-core forms in  $(V, X, k)$  when there exists some group of  $v$  vertices that exclusively share a set of at least  $2v$  edges. Define vertex set  $U$  such that  $|U| > |V|$ . Since the  $j$  edges in  $X$  are chosen uniformly at random, and there are more possible edges on vertex set  $U$ , the probability that a given set of  $2v$  edges forms in  $(U, X, k)$  must be lower than in  $(V, X, k)$ .

Fig. 9 shows the pseudocode for our algorithm, which relies on two functions. The function `decode( $j, k, c$ )` takes a random sample from the set of hypergraphs  $\mathcal{H}_{j,p}$  and determines if it forms a 2-core (i.e., if it decodes), returning `True` or `False`. The function `conf_int( $s, t$ )` returns the two-sided confidence interval of a proportion of  $s$  successes and  $t$  trials. We set  $c_{max} = 20$  in our implementation; in general, that value could be made part of the search itself [2]. In practice, we call Alg. 1 from an outer loop of values of  $k$  that we have observed to be reasonable (e.g., 3 to 12), and prune the search of each  $k$  when it is clear that it will not be smaller in size than a known result. To be clear, the algorithm is optimal within the values of  $k$  that are searched. Selecting a maximum value of  $k$  to search is an open problem, but we observe a trend that smaller  $k$  are better as  $j$  increases. See Bissias [4] for a related discussion.

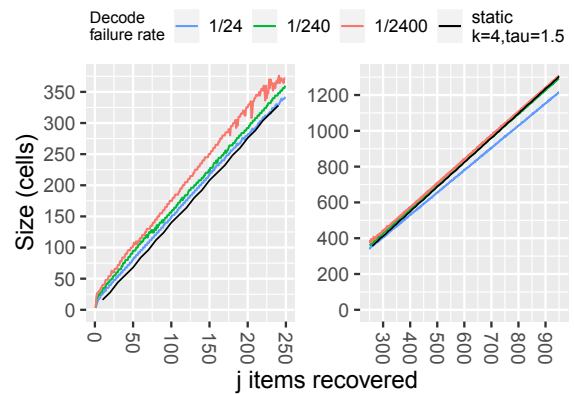


**Figure 10:** Size of optimal IBLTs (using Alg. 1) given a desired decode rate; with a statically parameterized IBLT ( $k = 4, \tau = 1.5$ ) in black. For clarity, the plot is split on the  $x$ -axis. Decode rates are shown in Fig. 7.

We have released an open-source implementation of IBLTs in C++ with a Python wrapper [36]. The release includes an implementation of Alg. 1 and optimal parameters for several decode rates. Although the runtime is linear with  $j$ , for any given rate, the parameter file can be generated once ever and be universally applicable to any IBLT implementation. Compared to a version of our algorithm that uses actual IBLTs, our hypergraph approach executes much faster for all  $j$ . For example, to parameterize  $j = 100$ , our approach completes in 29 seconds on average (100 trials). Allocating actual IBLTs increases average run time to 426 seconds. The speed increase is due to our use of hypergraphs, which are larger than IBLTs in terms of storage but are faster to compute with.

Fig. 10 shows the size of IBLTs when parameterized optimally for three different decode rates. If parameterized appropriately, the number of cells in an IBLT grows linearly, with variations due to inherent discretization and fewer degrees of freedom in small IBLTs.

## 4.2 Ping-Pong Decoding

Graphene takes advantage of its two IBLTs to increase the decode rate for Protocol 2. IBLTs **I** (and **I'**) and **J** (and **J'**) are different sizes, and may use a different number of hash functions, but contain the same transactions. When an IBLT fails to decode completely, it still can succeed partially. The transactions that are decoded from **J**  $\Delta$  **J'** can be removed from **I**  $\Delta$  **I'**, and decoding of the latter can be retried. Then, transactions from **I**  $\Delta$  **I'** can be removed from **J**  $\Delta$  **J'**, and decoding of the latter can be retried; and so on in a *ping-pong* fashion (see [28]). We note that if the count of a decoded item is 1, then it should be subtracted from the other IBLT; if the count is  $-1$ , then it should be added to the other IBLT. The IBLTs should use different seeds in their hash functions for independence.

Fig. 11 shows an experiment where we compared the decode rate of a single IBLT parameterized to be optimally small and recover  $j \in [10, 20, 50, 100]$  items with decode failure rate of  $1 - p = 1/240$ . We then inserted the same items into a second IBLT parameterized to hold  $0 < i \leq j$  items. When  $i$  is the same size as  $j$ , the failure rate is  $(1 - p)^2$  or lower. But improvements can be seen for values



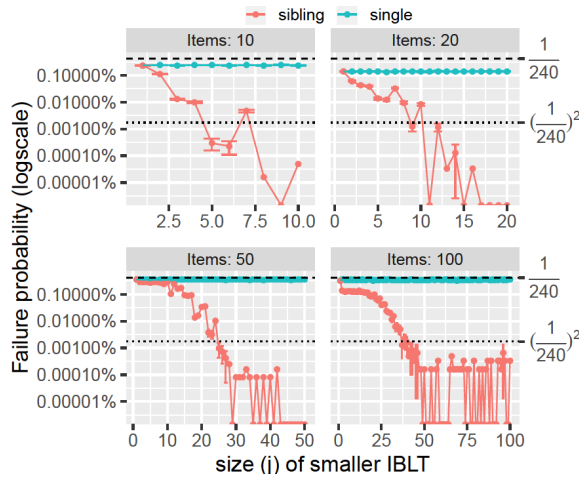


**Figure 11: Decode rate of a single IBLT (parameterized for a 1/240 failure rate) versus the improved ping-pong decode rate from using a second, smaller IBLT with the same items.**

$i < j$  as well. When  $j$  is small, very small values of  $i$  improve the decode rate. For larger values of  $j$ , larger values of  $i$  are needed for decoding. Ping-pong decoding is computationally fast since IBLT decoding itself is fast.

The use of ping-pong decoding on Graphene Protocol 2 is an improvement of several orders of magnitude; results are presented in Fig. 16 in Section 5.3.2.

This approach can be extended to other scenarios that we do not investigate here. For example, a receiver could ask many neighbors for the same block and the IBLTs can be jointly decoded with this approach.

## 5 EVALUATION

Our evaluation reaches the following conclusions:

- Graphene Protocol 1 is more efficient than using a Bloom filter alone, by  $\Omega(n \log n)$  bits. For all but small  $n$ , it is more efficient than deterministic solutions.
- We deployed Protocol 1 worldwide in Bitcoin Cash and show it performs as expected; and our implementation of Protocol 1 for Ethereum evaluated against historic data also shows expected gains.
- Using extensive Monte Carlo simulations, we show that Graphene Protocols 1 and 2 are always significantly smaller than Compact Blocks and XThin for a variety of scenarios, including mempool synchronization.
- In simulation, the decode success rates of Graphene Protocols 1 and 2 are above targeted values.

### 5.1 Comparison to Bloom Filter Alone

The information-theoretic bound on the number of bits required to describe any unordered subset of  $n$  elements, chosen from a set of  $m$  elements is  $\lceil \log_2 \binom{m}{n} \rceil \approx n \log_2(m/n)$  bits [11]. Carter et al. also showed that an approximate solution to the problem has a more efficient lower bound of  $-n \log_2(f)$  bits by allowing for a false positive rate of  $f$  [14].

Because our goal is to address a restricted version of this problem, Graphene Protocol 1 is more efficient than Carter’s bound for even an optimal Bloom filter alone. This is because Graphene Protocol 1 assumes all  $n$  elements (transactions) are stored at the receiver, and makes use of that information whereas a Bloom filter would not.

**THEOREM 4:** *Relaying a block with  $n$  transactions to a receiver with a mempool (a superset of the block) of  $m$  transactions is more efficient with Graphene Protocol 1 than using an optimally small Bloom filter alone, when the IBLT uses  $k \geq 3$  hash functions. The efficiency gains of Graphene Protocol 1 are  $\Omega(n \log_2 n)$ .*

A full proof appears in Appendix B. Graphene cannot replace all uses of Bloom filters, only those where the elements are stored at the receiver, e.g., set reconciliation.

As  $m - n$  approaches zero, Protocol 1 shrinks its Bloom filter and approaches an IBLT-only solution. The special case where Graphene has an FPR of 1 is equivalent to not sending a Bloom filter at all; in that case, Graphene is as small as any IBLT-only solution, as expected. As the size of  $m - n$  increases, Graphene is much smaller than sticking with an IBLT-only solution, which would have  $\tau(m - n)$  cells.

Graphene is not always smaller than deterministic solutions. As we show in our evaluations below, for small values of  $n$  (about 50–100 or fewer depending on constants), deterministic solutions perform better. For larger values, Graphene’s savings are significant and increase with  $n$ .

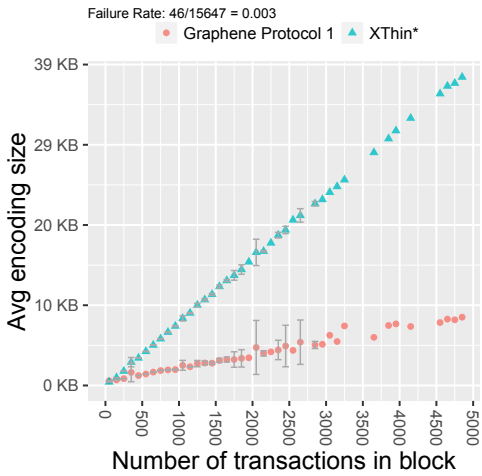
We leave analytic claims regarding Protocol 2 for future work; however, below we empirically demonstrate its advantage over related work.

### 5.2 Implementations

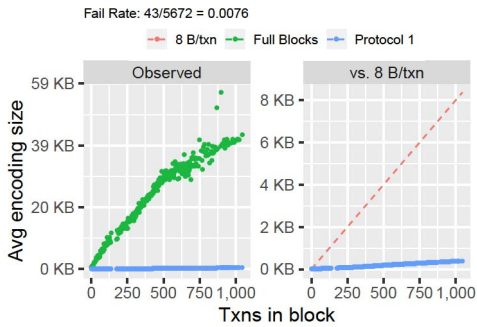
**Bitcoin Cash implementation.** We coded Graphene (Protocol 1) for Bitcoin Unlimited’s Bitcoin Cash client. It appeared first in edition 1.4.0.0 (Aug 17, 2018) as an experimental feature, and since 1.5.0.1 (Nov 5, 2018) it has been the default block propagation technique. Currently, 686 nodes (operated by persons unknown to us) are running Graphene on the Bitcoin Cash mainnet.

Fig. 12 shows results from our own peer running the protocol on the real network from January 9–April 29, 2019. Fig. 12 also shows results from using Bitcoin Unlimited’s XThin implementation; however, we have removed the cost of the receiver’s Bloom filter to make the comparison fair (hence it is labelled XThin\*). The cost of XThin\* is computed for the same blocks. As expected, while XThin\* costs grow quickly, the costs of Graphene grow much more slowly as block size increases.

We have not yet deployed Protocol 2 (below we discuss our simulation of Protocol 2). Out of 15,647 Graphene blocks, 46 failed to decode, which is within our  $\beta$ -assurance of 239/240. This statistic also confirms our two-protocol approach: most of the time Protocol 1 is sufficient; and correcting failures with Protocol 2 is rarely needed if  $\beta$  is set appropriately. And although the failure rate of Protocol 1 is low, Protocol 2 is a necessary part of a complete solution for our probabilistic approach.



**Figure 12: [Deployment on BCH, Protocol 1]: Performance of Protocol 1 as deployed on the Bitcoin Cash network, where the node was connected to 6 other peers. Points are averages of binned sizes; error bars show 95% c.i. if at least 3 blocks of that size can be averaged.**



**Figure 13: [Implementation, Protocol 1] An implementation of Protocol 1 for the Geth Ethereum client run on historic data. The left facet compares against Ethereum’s use of full blocks; the right compares against an idealized version of Compact Blocks using 8 bytes/transaction.**

**Ethereum implementation.** We implemented Graphene Protocol 1 for *Geth*, Ethereum’s primary client software, and submitted a Pull Request [31]. We replayed all the blocks produced on the Ethereum mainnet blockchain on Jan 14, 2019 (a total of 5,672 blocks), introducing new message types to comply with Graphene’s protocol. During our test, the size of the mempool at the receiver was kept constant at 60,000 transactions, which is typical (see <https://etherscan.io/chart/pendingtx>). The left facet of Fig. 13 shows the size in bytes of full blocks used by Ethereum and Graphene. The right facet compares Graphene (including transaction ordering information) against a line showing 8 bytes/per transaction (an idealization of Compact Blocks without overhead).

### 5.3 Monte Carlo Simulation

**Methodology and assumptions.** We also wrote a custom block propagation simulator for Graphene (Protocols 1 and 2) that measures the network bytes exchanged by peers relating blocks. We executed the protocol using real data structures so that we could

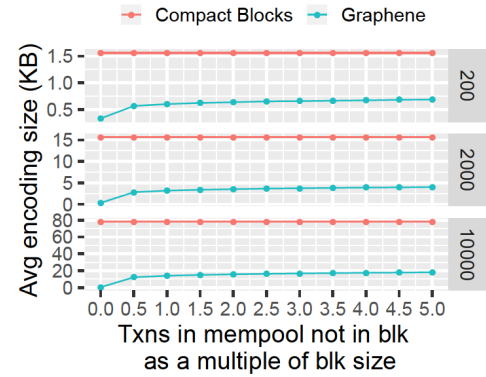


**Figure 14: [Simulation, Protocol 1] Average size of Graphene blocks versus Compact Blocks as the size of the mempool increases as a multiple of block size. Each facet is a block size: (200, 2000, and 10000 transactions). (N.b., This figure varies mempool size; Fig. 12 varied block size.)**

capture the probabilistic nature of Bloom filters and IBLTs. Specifically, we used our publicly released IBLT implementation and a well-known Python Bloom filter implementation. In results below, we varied several key parameters, including the size of the block, the size of the receiver’s mempool, and the fraction of the block possessed at the receiver. Each point in our plots is one parameter combination and shows the mean of 10,000 trials or more; if no confidence interval is shown, it was very small and removed for clarity. For all trials, we used a bound of  $\beta = 239/240$  (see Eqs. 7 and 10).

In all experiments, we evaluated three block sizes (in terms of transactions): 200, which is about the average size of Ethereum (ETH) and Bitcoin Cash (BCH) blocks; 2,000 which is the average size of Bitcoin (BTC) blocks; and 10,000 as an example of a larger block scenario. In expectation of being applied to large blocks and mempools, we used 8-byte transaction IDs for both Graphene and Compact Blocks. Also for Compact Blocks, we used `getdata` messages with block encodings of 1 or 3 bytes, depending on block size [15].

#### 5.3.1 Graphene: Protocol 1.

**Size of blocks.** Fig. 14 shows the cost in bytes of Graphene blocks compared to Compact Blocks. We focus on varying mempool size rather than block size. In these experiments, the receiver’s mempool contains all transactions in the block plus some additional transactions, which increase along the x-axis as a multiple of the block size. For example, at fraction 0.5 and block size 2,000, the mempool contains 3,000 transactions in total. The experiments demonstrate that Graphene’s advantage over Compact Blocks is substantial and improves with block size. Also, the cost of Graphene grows sublinearly as the number of extra transactions in the mempool grows.

**Decode rate.** Fig. 15 shows the decode rate of Graphene blocks, as the mempool size increases. In all cases, the decode rate far exceeds the desired rate, demonstrating that our derived bounds are effective. Graphene’s decode rate suffers when the receiver lacks the entire block in her mempool. For example, in our experiments,

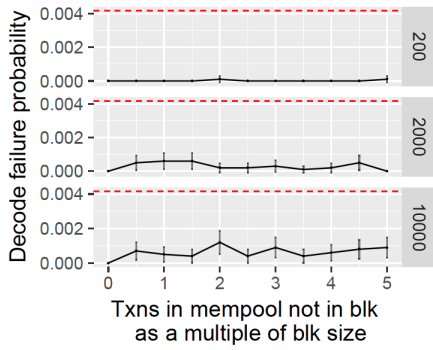


Figure 15: [Simulation, Protocol 1] Decode rate of Graphene blocks with  $\beta = \frac{239}{240}$  (red dotted line), as block size and the number of extra transactions in the mempool increases as a multiple of block size.

a receiver holding 99% of the block can still decode 97% of the time. But if the receiver holds less than 98% of the block, the decode rate for Protocol 1 is zero. Hence, Protocol 2 is required in such scenarios.

5.3.2 Graphene Extended: Protocol 2.

Our evaluations of Protocol 2 focus on scenarios where the receiver does not possess the entire block and  $m > n$ ; we evaluate  $m = n$  as a special case.

**Size by message type.** Fig. 17 shows the cost of Graphene Extended, broken down into message type, as the fraction of the block owned by the receiver increases. The dashed line on the plot shows the costs for Compact Blocks, where the receiver requests missing transactions by identifying each as a 1- or 3-byte index (depending on block size) in the original ordered list of transactions in the block encodings [15]. (We exclude the cost of sending the missing transactions themselves for both protocols.)

Overall, Graphene Extended is significantly smaller than Compact Blocks, and the gains increase as the block size increases. For blocks smaller than 200, eventually Compact Blocks would be smaller in some scenarios.

**Decode rate and Ping-Pong enhancement.** Fig. 16 shows the decode rate of Graphene blocks; it far exceeds the desired rate. And when ping-pong decoding is used, the simulation results show decoding rates close to 100%.

Not shown are our simulations of the Difference Digest by Epstein et al. [23]. The Difference Digest is an IBLT-only solution that is an alternative to our Protocol 2. In that work, the sender begins by telling the receiver the value  $n$ . The receiver creates a Flajolet-Martin estimate [26] of  $m - n$ , using  $\lceil \log_2(m - n) \rceil$  IBLTs, each with 80 cells where roughly  $m$  elements are inserted. The sender replies with a single IBLT of twice the number of cells as the estimate (to account for an under-estimate). This approach is several times more expensive than Graphene.

**$m \approx n$  and mempool synchronization.** As described in Section 3.2.1, Graphene can be used for mempool synchronization, setting  $n$  to the size of the sender’s mempool. In these cases, if peers are mostly synchronized, then  $m \approx n$ , which is a special case for Graphene

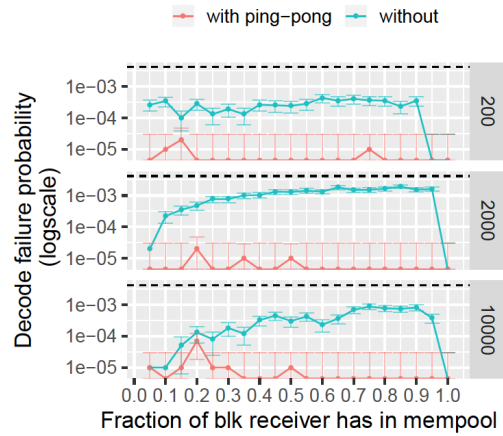


Figure 16: [Simulation, Protocol 2] Decode rate of Graphene blocks with  $\beta = \frac{239}{240}$ , shown by the black dotted line, as block size and the number of extra transactions in the mempool increase. Error bars represent 95% confidence intervals.

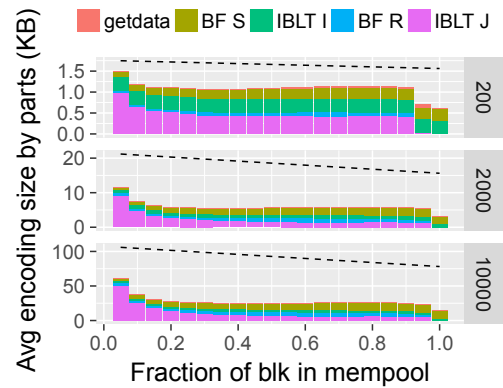


Figure 17: [Simulation, Protocol 2] Graphene Extended cost as the fraction of the block owned by the receiver increases. The black dotted line is the cost of Compact Blocks.

discussed in Section 3.3.1. Our evaluations of this scenario are shown in Fig. 18. In these experiments, the sender’s mempool has  $n$  transactions, of which a fraction (on the x-axis) are in common with the receiver. The receiver’s mempool size is topped off with unrelated transactions so that  $m = n$ . As a result, Protocol 1 fails and modifications from Section 3.3.1 are employed. As with previous experiments, Graphene performs significantly better than Compact Blocks across multiple mempool intersection sizes and improvement increases with block size.

6 SYSTEMS ISSUES

6.1 Security Considerations

**Malformed IBLTs.** It is simple to produce an IBLT that results in an endless decode loop for a naive implementation; the attack is just as easily thwarted. To create a malformed IBLT, the attacker

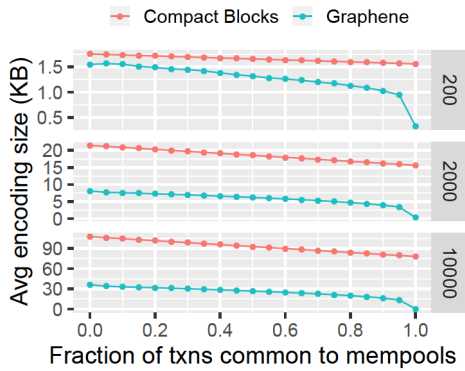


**Figure 18: [Simulation, Mempool Synchronization]** Here  $m = n$  and the peers have a fraction of the sender’s mempool in common on the x-axis. Graphene is more efficient, and the advantage increases with block and mempool size.

incorrectly inserts an item into only  $k - 1$  cells. When the item is peeled off, one cell in the IBLT will contain the item with a count of -1. When that entry is peeled,  $k - 1$  cells will contain the item with a count of 1; and the loop continues. The attack is thwarted if the implementation halts decoding when an item is decoded twice. Once detected, the sender can be dropped or banned by the receiver.

**Manufactured transaction collisions.** The probability of accidental collision of two 8-byte transaction IDs in a mempool of size  $m$  is  $\approx 1 - \text{Exp}\left(\frac{-m(m-1)}{265}\right)$  [43]. An attacker may use brute force search to discover and submit collisions. SipHash [1] is used by some blockchain protocols to limit the attack to a single peer.

With or without the use of SipHash, Graphene is more resilient against such collisions than XThin and Compact Blocks. Let  $t_1$  and  $t_2$  be transactions with IDs that collide with at least 8 bytes. In the worst case, the block contains  $t_1$ , the sender has never seen  $t_2$ , and the receiver possesses  $t_2$  but has never seen  $t_1$ . In this case, XThin and Compact Blocks will always fail; however, Graphene fails with low probability,  $f_S \cdot f_R$ . For the attack to succeed, first,  $t_2$  must pass through Bloom filter  $\mathbf{S}$  as a full 32-byte ID, which occurs only with probability  $f_S$ . If it does pass, the IBLT will decode but the Merkle root will fail. At this point, the receiver will initiate Protocol 2, sending Bloom filter  $\mathbf{R}$ . Second, with probability  $f_R$ ,  $t_1$  will be a false positive in  $\mathbf{R}$  as a full 32-byte ID and will not be sent to the receiver.

## 6.2 Transaction Ordering Costs

Bloom filters and IBLTs operate on unordered sets, but Merkle trees require a specific ordering. In our evaluations, we did not include the sender’s cost of specifying a transaction ordering, which is  $n \log_2 n$  bits. As  $n$  grows, this cost is larger than Graphene itself. Fortunately, the cost is easily eliminated by introducing a known ordering of transactions in blocks. In fact, Bitcoin Cash clients deployed a Canonical Transaction Ordering (CTOR) ordering in Fall 2018.

## 6.3 Reducing Processing Time

Profiling our implementation code revealed that processing costs are dominated heavily by passing the receiver’s mempool against Bloom filter  $\mathbf{S}$  in Protocol 1. Fortunately, this cost is easily reduced. A standard Bloom filter implementation will hash each transaction ID  $k$  times — but each ID is already the result of applying a cryptographic hash and there is no need to hash  $k$  more times; see Suisani et al. [50]. Instead, we break the 32-byte transaction ID into  $k$  pieces. Applying this solution reduced average receiver processing in our Ethereum implementation from 17.8ms to 9.5ms. Alternative techniques [19, 20, 32] are also effective and not limited to small values of  $k$ .

## 6.4 Limitations

Graphene is a solution for set reconciliation where there is a trade-off between transmission size, complexity (in terms of network round-trips), and success rate. In contrast, popular alternatives such as Compact Blocks [15] have predictable transmission size, fixed transmission complexity, use a trivial algorithm, and always succeed. Graphene’s performance gains over related work increase as block size grows, but it is a probabilistic solution with a (tunable) failure rate. We do not claim to have the optimal solution for propagating blocks, nor for scaling blockchains in general.

## 7 CONCLUSIONS

We introduced a novel solution to the problem of determining a subset of items from a larger set two parties hold in common, using a novel combination of Bloom filters and IBLTs. We also provided a solution to the more general case, where one party is missing some or all of the subset. Specifically, we described how to parametrize the probabilistic data structures in order to meet a desired decode rate. Through a detailed evaluation using simulations and real-world deployment, we compared our method to existing systems, showing that it requires less data transmission over a network and is more resilient to attack than previous approaches.

**Acknowledgements.** We are grateful for insightful help from Awe-many, Srikanth Kandula, Andrew Stone, Andrea Suisani, and Peter Tschipper. This work was funded in part by Bitcoin Unlimited, and it was performed in part using high performance computing equipment obtained under a grant from the Collaborative R&D Fund managed by the Massachusetts Technology Collaborative.

## REFERENCES

- [1] Jean-Philippe Aumasson and Daniel J. Bernstein. (December 2012). SipHash: A Fast Short-Input PRF. In *Proc. Progress in Cryptology (INDOCRYPT)*. 489–508.
- [2] Jon Louis Bentley and Andrew Chi-Chih Yao. 1976. An almost optimal algorithm for unbounded searching (see also [https://en.wikipedia.org/wiki/Exponential\\_search](https://en.wikipedia.org/wiki/Exponential_search)). *Information Processing Letters*. 5, 3 (Aug 1976), 82–87. [https://doi.org/10.1016/0020-0190\(76\)90071-5](https://doi.org/10.1016/0020-0190(76)90071-5)
- [3] George Bissias. 2018. Graphene Pull Request. <https://github.com/BitcoinUnlimited/BitcoinUnlimited/pull/973>. (July 2018).
- [4] George Bissias. 2019. An Algorithm for Bounding the Probability of  $r$ -core Formation in  $k$ -uniform Random Hypergraphs. arXiv preprint. (Feb 1 2019). <http://arxiv.org/abs/1901.04934>
- [5] George Bissias and Brian Levine. 2018. BUIP093: Graphene Relay. <https://github.com/BitcoinUnlimited/BUIP/blob/master/093.mediawiki>. (July 26 2018).
- [6] Bitcoin ABC. 2018. The Bitcoin ABC Vision. [https://medium.com/@Bitcoin\\_ABC/the-bitcoin-abc-vision-f7f87755979f](https://medium.com/@Bitcoin_ABC/the-bitcoin-abc-vision-f7f87755979f). (August 24 2018).

- [7] Bitcoin Unlimited. 2018. Bitcoin Cash Development And Testing Accord: Bitcoin Unlimited Statement. <https://www.bitcoinunlimited.info/cash-development-plan>. (2018).
- [8] Burton H. Bloom. 1970. Space/Time Trade-offs in Hash Coding with Allowable Errors. *Commun. ACM* 13, 7 (July 1970), 422–426.
- [9] Anudhyan Boral and Michael Mitzenmacher. (October 2014). Multi-Party Set Reconciliation Using Characteristic Polynomials. In *Proc. Annual Allerton Conference on Communication, Control, and Computing*. 1182–1187.
- [10] Andrei Broder and Michael Mitzenmacher. 2004. Network applications of bloom filters: A survey. *Internet mathematics* 1, 4 (2004), 485–509.
- [11] Andrej Brodnik and Jan Jan Munro. 1999. Membership in constant time and almost-minimum space. *SIAM J. Comput.* 28, 5 (1999), 1627–1640.
- [12] Vitalik Buterin and Virgil Griffith. 2017. Casper the Friendly Finality Gadget. <https://arxiv.org/abs/1710.09437>. (Oct 2017).
- [13] John W Byers, Jeffrey Considine, Michael Mitzenmacher, and Stanislav Rost. 2004. Informed content delivery across adaptive overlay networks. *IEEE/ACM transactions on networking* 12, 5 (2004), 767–780.
- [14] Larry Carter, Robert Floyd, John Gill, George Markowsky, and Mark Wegman. (1978). Exact and Approximate Membership Testers. In *Proceedings of the Tenth Annual ACM Symposium on Theory of Computing*. ACM, 59–65. <http://doi.acm.org/10.1145/800133.804332>
- [15] Matt Corallo. 2016. BIP152: Compact Block Relay. <https://github.com/bitcoin/bips/blob/master/bip-0152.mediawiki>. (April 2016).
- [16] Kyle Croman, Christian Decker, Ittay Eyal, Adem Efe Gencer, Ari Juels, Ahmed Kosba, Andrew Miller, Prateek Saxena, Elaine Shi, Emin Gün Sirer, Dawn Song, and Roger Wattenhofer. (February 2016). On Scaling Decentralized Blockchains. In *Proc. Financial Cryptography and Data Security*. 106–125.
- [17] George Danezis and Sarah Meiklejohn. (February 2016). Centrally Banked Cryptocurrencies. In *Proc. Network and Distributed System Security Symposium (NDSS)*. 14 pages. <https://doi.org/10.14722/ndss.2016.23187>
- [18] Christian Decker and Roger Wattenhofer. (September 2013). Information Propagation in the Bitcoin Network. In *Proc. IEEE International Conference on Peer-to-Peer Computing*. 1–10.
- [19] Peter C. Dillinger and Panagiotis Manolios. (November 2004). Bloom Filters in Probabilistic Verification. In *Proc. International Conference on Formal Methods in Computer-Aided Design (FMCAD)*. Springer-Verlag, 367–381.
- [20] Peter C. Dillinger and Panagiotis Manolios. (April 2004). Fast and Accurate Bitstate Verification for SPIN. In *Proc. Model Checking Software (SPIN)*. 57–75. [https://doi.org/10.1007/978-3-540-24732-6\\_5](https://doi.org/10.1007/978-3-540-24732-6_5)
- [21] Yevgeniy Dodis, Rafail Ostrovsky, Leonid Reyzin, and Adam Smith. 2008. Fuzzy Extractors: How to Generate Strong Keys from Biometrics and Other Noisy Data. *SIAM journal on computing* 38, 1 (2008), 97–139.
- [22] Thaddeus Dryja and Joseph Poon. 2016. The Bitcoin Lightning Network: Scalable Off-Chain Instant Payments. <https://lightning.network/lightning-network-paper.pdf>. (Jan 2016).
- [23] David Eppstein, Michael T. Goodrich, Frank Uyeda, and George Varghese. (August 2011). What's the Difference? Efficient Set Reconciliation Without Prior Context. In *Proc. ACM SIGCOMM*. 218–229.
- [24] Bin Fan, Dave G. Andersen, Michael Kaminsky, and Michael D. Mitzenmacher. (December 2014). Cuckoo Filter: Practically Better Than Bloom. In *Proc. ACM International Conference on emerging Networking Experiments and Technologies (CoNEXT)*. 75–88. <https://doi.org/10.1145/2674005.2674994>
- [25] Michael Fischer, Nancy Lynch, and Michael Paterson. 1985. Impossibility of distributed consensus with one faulty process. *JACM* 32, 2 (1985), 374–382.
- [26] Philippe Flajolet and G. Nigel Martin. 1985. Probabilistic counting algorithms for data base applications. *J. Comput. System Sci.* 31, 2 (1985), 182–209. [https://doi.org/10.1016/0022-0000\(85\)90041-8](https://doi.org/10.1016/0022-0000(85)90041-8)
- [27] Yossi Gilad, Rotem Hemo, Silvio Micali, Georgios Vlachos, and Nickolai Zeldovich. (October 2017). Algorand: Scaling Byzantine Agreements for Cryptocurrencies. In *Proc. Symposium on Operating Systems Principles (SOSP)*. 51–68.
- [28] Shyamnath Gollakota and Dina Katabi. (August 2008). Zigzag Decoding: Combating Hidden Terminals in Wireless Networks. In *Proc. ACM SIGCOMM Conference on Data Communication*. 159–170. <https://doi.org/10.1145/1402958.1402977>
- [29] Solomon W. Golomb. 1966. Run-length encodings (Corresp.). *IEEE Transactions on Information Theory* 12, 3 (July 1966), 399–401. <https://doi.org/10.1109/TIT.1966.1053907>
- [30] Michael Goodrich and Michael Mitzenmacher. (Sept 2011). Invertible bloom lookup tables. In *Conf. on Comm., Control, and Computing*. 792–799.
- [31] Sunny Katkuri. 2018. Improve block transfer efficiency using Graphene #17724. <https://github.com/ethereum/go-ethereum/pull/17724>. (September 20 2018).
- [32] Adam Kirsch and Michael Mitzenmacher. 2006. Less Hashing, Same Performance: Building a Better Bloom Filter. *Random Structures & Algorithms* 33, 2 (September 2006), 187–218. <https://doi.org/10.1002/rsa.20208>
- [33] Eleftherios Kokoris Kogias, Philipp Jovanovic, Nicolas Gailly, Ismail Khoffi, Linus Gasser, and Bryan Ford. (August 2016). Enhancing Bitcoin Security and Performance with Strong Consistency via Collective Signing. In *Proc. USENIX Security Symposium*. 279–296.
- [34] Eleftherios Kokoris-Kogiasy, Philipp Jovanovic, Linus Gassery, Nicolas Gailly, Ewa Syta, and Bryan Ford. (May 2018). OmniLedger: A Secure, Scale-Out, Decentralized Ledger via Sharding. In *Proc. IEEE Symposium on Security and Privacy*. 583–598.
- [35] James Larisch, David Choffnes, Dave Levin, Bruce M Maggs, Alan Mislove, and Christo Wilson. (May 2017). CRLite: A Scalable System for Pushing All TLS Revocations to All Browsers. In *Proc. IEEE Symposium on Security and Privacy*. 539–556.
- [36] Brian Levine and Gavin Andresen. 2018. IBLT Optimization. <https://github.com/umass-forensics/IBLT-optimization>. (August 2018).
- [37] Yoad Lewenberg, Yonatan Sompolinsky, and Aviv Zohar. (Jan 2015). Inclusive block chain protocols. In *Proc. International Conference on Financial Cryptography and Data Security*. 528–547.
- [38] Eric Russell Love. 1980. Some Logarithm Inequalities. *The Mathematical Gazette (The Mathematical Association)* 63, 427 (March 1980), 55–57. <https://www.jstor.org/stable/3615890>
- [39] Lailong Luo, Deke Guo, Richard T.B. Ma, Ori Rottenstreich, and Xueshan Luo. 2019. Optimizing Bloom Filter: Challenges, Solutions, and Comparisons. *IEEE Communications Surveys Tutorials* (see also arXiv:1804.04777) 21, 2 (Second quarter 2019), 1912–1949.
- [40] Ralph C. Merkle. (1987). A Digital Signature Based on a Conventional Encryption Function. In *Advances in Cryptology (CRYPTO '87)*. August, 369–378. [https://doi.org/10.1007/3-540-48184-2\\_32](https://doi.org/10.1007/3-540-48184-2_32)
- [41] Yaron Minsky, Ari Trachtenberg, and Richard Zippel. 2003. Set reconciliation with nearly optimal communication complexity. *IEEE Transactions on Information Theory* 49, 9 (2003), 2213–2218.
- [42] Michael Mitzenmacher and Rasmus Pagh. 2018. Simple multi-party set reconciliation. *Distributed Computing* 31, 6 (November 2018), 441–453.
- [43] Michael Mitzenmacher and Eli Upfal. 2005. *Probability and Computing: Randomized Algorithms and Probabilistic Analysis*. Cambridge University Press. 61–89 pages. <https://doi.org/10.1017/CBO9780511813603.005>
- [44] Michael Molloy. (January 2004). The Pure Literal Rule Threshold and Cores in Random Hypergraphs. In *Proc. ACM-SIAM Symposium on Discrete Algorithms (SODA)*. 672–681. <http://dl.acm.org/citation.cfm?id=982792.982896>
- [45] Satoshi Nakamoto. 2009. Bitcoin: A Peer-to-Peer Electronic Cash System. (May 2009). <https://bitcoin.org/bitcoin.pdf>
- [46] A. Pinar Ozisik, Gavin Andresen, George Bissias, Amir Houmansadr, and Brian Neil Levine. (September 2017). Graphene: A New Protocol for Block Propagation Using Set Reconciliation. In *Proc. of International Workshop on Cryptocurrencies and Blockchain Technology (ESORICS Workshop)*. 420–428.
- [47] Salvatore Pontarelli, Pedro Reviriego, and Michael Mitzenmacher. 2014. Improving the performance of Invertible Bloom Lookup Tables. *Inform. Process. Lett.* 114, 4 (2014), 185–191. <https://doi.org/10.1016/j.ipl.2013.11.015>
- [48] Stephen B. Seidman. 1983. Network structure and minimum degree. *Social Networks* 5, 3 (1983), 269–287. [https://doi.org/10.1016/0378-8733\(83\)90028-X](https://doi.org/10.1016/0378-8733(83)90028-X)
- [49] Yonatan Sompolinsky and Aviv Zohar. (January 2015). Secure high-rate transaction processing in Bitcoin. In *Proc. Financial Cryptography and Data Security*. 507–527.
- [50] Andrea Suisani, Andrew Clifford, Andrew Stone, Erik Beijnoff, Peter Rizun, Peter Tschipper, Alexandra Fedorova, Chen Feng, Victoria Lemieux, and Stefan Matthews. (November 2017). Measuring maximum sustained transaction throughput on a global network of Bitcoin nodes. [https://scalingbitcoin.org/stanford2017/Day1/Stanford\\_2017.pptx.pdf](https://scalingbitcoin.org/stanford2017/Day1/Stanford_2017.pptx.pdf). In *Proc. Scaling Bitcoin Conference*.
- [51] Sasu Tarkoma, Christian Esteve Rothenberg, and Eemil Lagerspetz. 2012. Theory and Practice of Bloom Filters for Distributed Systems. *IEEE Communications Surveys Tutorials* 14, 1 (First 2012), 131–155. <https://doi.org/10.1109/SURV.2011.031611.00024>
- [52] Jonathan Toomim. 2018. Benefits of LTOR in block entropy encoding. [https://medium.com/@j\\_73307/benefits-of-ltor-in-block-entropy-encoding-or-8d5b77cc2ab0](https://medium.com/@j_73307/benefits-of-ltor-in-block-entropy-encoding-or-8d5b77cc2ab0). (September 2018).
- [53] Jonathan Toomim. 2018. Block propagation data from Bitcoin Cash's stress test. [https://medium.com/@j\\_73307/block-propagation-data-from-bitcoin-cashs-stress-test-5b1d7d39a234](https://medium.com/@j_73307/block-propagation-data-from-bitcoin-cashs-stress-test-5b1d7d39a234). (September 2018).
- [54] Peter Tschipper. 2016. BUIP010 Xtreme Thinblocks. <https://bitco.in/forum/threads/buip010-passed-xtreme-thinblocks.774/>. (Jan 2016).
- [55] Gavin Wood. 2018. Ethereum: A Secure Decentralised Generalised Transaction Ledger. <https://ethereum.github.io/yellowpaper/paper.pdf>. (June 2018).
- [56] Pieter Wuille. 2018. Minisketch: a library for BCH-based set reconciliation. <https://github.com/sipa/minisketch/blob/master/doc/math.md>. (2018).

*Required statement:* Appendices are supporting material that has not been peer reviewed.

## A THEOREMS FROM SECTION 3.3

For completeness, we provide the proof of a well-known version of Chernoff bounds that appears commonly in lecture notes, but not in any formal reference to our knowledge.

**LEMMA 1:** Let  $A$  be the sum of  $i$  independent Bernoulli trials  $A_1, \dots, A_i$ , with mean  $\mu = E[A]$ . Then for  $\delta > 0$

$$\Pr[A \geq (1 + \delta)\mu] \leq \text{Exp}\left(-\frac{\delta^2}{2 + \delta}\mu\right),$$

**PROOF:** Starting from the well-known Chernoff bound [43]:

$$\begin{aligned} \Pr[A \geq (1 + \delta)\mu] &\leq \left(\frac{e^\delta}{(1 + \delta)^{1 + \delta}}\right)^\mu \\ &= \text{Exp}(\mu(\delta - (1 + \delta)\ln(1 + \delta))) \\ &\leq \text{Exp}\left(\mu\left(\delta - (1 + \delta)\left(\frac{2\delta}{2 + \delta}\right)\right)\right) \\ &= \text{Exp}\left(\frac{-\delta^2}{2 + \delta}\mu\right) \end{aligned}$$

Above, we rely on the inequality  $\ln(1 + x) \geq \frac{x}{1 + x/2} = \frac{2x}{2 + x}$  for  $x > 0$  (see [38]), and that  $e^{a-b} \leq e^{a-c}$  when  $b \geq c$ .  $\square$

**THEOREM 1:** Let  $m$  be the size of a mempool that contains all  $n$  transactions from a block. If  $a$  is the number of false positives that result from passing the mempool through Bloom filter  $\mathbf{S}$  with FPR  $f_S$ , then  $a^* \geq a$  with probability  $\beta$  when

$$\begin{aligned} a^* &= (1 + \delta)a, \\ \text{where } \delta &= \frac{1}{2}(s + \sqrt{s^2 + 8s}) \text{ and } s = \frac{-\ln(1 - \beta)}{a}. \end{aligned}$$

**PROOF:** There are  $m - n$  potential false positives that pass through  $\mathbf{S}$ . They are a set  $A_1, \dots, A_{m-n}$  of independent Bernoulli trials such that  $\Pr[A_i = 1] = f_S$ . Let  $A = \sum_{i=1}^{m-n} A_i$  and  $\mu = E[A] = f_S(m - n) = \frac{a}{m-n}(m - n) = a$ . From Lemma 1, we have

$$\Pr[A \geq (1 + \delta)\mu] \leq \text{Exp}\left(-\frac{\delta^2}{2 + \delta}\mu\right),$$

for  $\delta \geq 0$ . The receiver can set a bound of choice,  $0 < \beta < 1$ , and solve for  $\delta$  using the right hand side of the above equation. To bound with high probability, we seek the complement of the right hand side

$$\begin{aligned} \beta &= 1 - \text{Exp}\left(-\frac{\delta^2}{2 + \delta}a\right) \\ \delta &= \frac{1}{2}(s + \sqrt{s^2 + 8s}), \text{ where } s = \frac{-\ln(1 - \beta)}{a}. \end{aligned} \quad (7)$$

**THEOREM 2:** Let  $m$  be the size of a mempool containing  $0 \leq x \leq n$  transactions from a block. Let  $z = x + y$  be the count of mempool transactions that pass through  $\mathbf{S}$  with FPR  $f_S$ , with true positive count  $x$  and false positive count  $y$ . Then  $x^* \leq x$

with probability  $\beta$  when

$$x^* = \arg \min_{x^*} \Pr[x \leq x^*; z, m, f_S] \leq 1 - \beta.$$

$$\text{where } \Pr[x \leq k; z, m, f_S] \leq \sum_{i=0}^k \left(\frac{e^{\delta_k}}{(1 + \delta_k)^{1 + \delta_k}}\right)^{(m-k)f_S}$$

$$\text{and } \delta_k = \frac{z - k}{(m - k)f_S} - 1.$$

**PROOF:** Let  $Y_1, \dots, Y_{m-x}$  be independent Bernoulli trials representing transactions not in the block that might be false positives; i.e.,  $\Pr[Y_i = 1] = f_S$ . We have  $y = E[Y]$  and  $Y = \sum_{i=1}^{m-x} Y_i$ .

For a given value  $x$ , we can compute  $\Pr[Y \geq y]$ , the probability of at least  $y$  false positives passing through the sender's Bloom filter. We apply a Chernoff bound [43]:

$$\Pr[y; z, x, m] = \Pr[Y \geq (1 + \delta)\mu] \leq \left(\frac{e^\delta}{(1 + \delta)^{1 + \delta}}\right)^\mu \quad (8)$$

where  $\delta > 0$ , and  $\mu = E[Y] = (m - x)f_S$ . By setting  $(1 + \delta)\mu = z - x$  and solving for  $\delta$ , we have

$$\begin{aligned} (1 + \delta)(m - x)f_S &= z - x \\ \delta &= \frac{z - x}{(m - x)f_S} - 1. \end{aligned}$$

We substitute  $\delta$  into Eq. 8 and bound the probability of observing a value of  $y = z - x$  or greater, given that the receiver has  $x$  transactions in the block. This realization allows us to enumerate all possible scenarios for observation  $z$ . The cumulative probability of observing  $y$ , parametrized by  $z$ , given that the receiver has at most  $k$  of the transactions in the block, is:

$$\begin{aligned} \Pr[x \leq k; z, m, f_S] &= \sum_{i=0}^k \Pr[y; z, k, m] \\ &\leq \sum_{i=0}^k \left(\frac{e^{\delta_k}}{(1 + \delta_k)^{1 + \delta_k}}\right)^{(m-k)f_S} \end{aligned}$$

where  $\delta_k = \frac{z - k}{(m - k)f_S} - 1$ . Finally, using this closed-form equation, we select a bounding probability  $\beta$ , such as  $\beta = 239/240$ . We seek a probability  $\beta$  of observing  $z$  from a value  $x^*$  or larger; equivalently, we solve for the complement:

$$\arg \min_{x^*} \Pr[x \leq x^*; z, m, f_S] \leq 1 - \beta.$$

To summarize,  $x^*$  is the *smallest* number of true positives such that the cumulative probability of observing  $y = z - x^*$  false positives is at least  $1 - \beta$ .  $\square$

For good measure, we validated the theorem empirically, as shown in Fig. 19.

**THEOREM 3:** Let  $m$  be the size of a mempool containing  $0 \leq x \leq n$  transactions from a block. Let  $z = x + y$  be the count of mempool transactions that pass through  $\mathbf{S}$  with FPR  $f_S$ , with true positive count  $x$  and false positive count  $y$ . Then  $y^* \geq y$

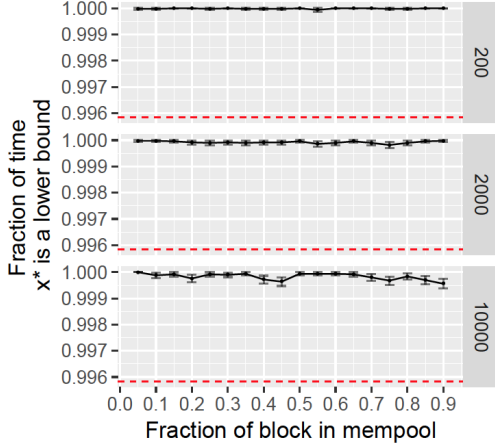


Figure 19: [Simulation, Protocol 2] The fraction of Monte Carlo experiments where  $x^* < x$  via Theorem 2 compared to a desired bound of  $\beta = 239/240$  (shown as a red dotted line).

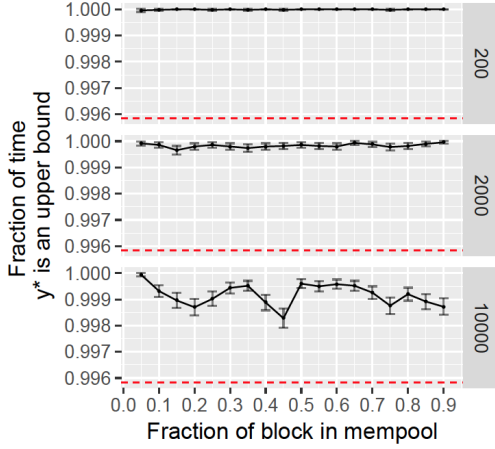


Figure 20: [Simulation, Protocol 2] The fraction of Monte Carlo experiments where  $y^* > y$  via Theorem 3 compared to a desired bound of  $\beta = 239/240$  (shown as a red dotted line).

with probability  $\beta$  when

$$y^* = (1 + \delta)(m - x^*)f_S,$$

$$\text{where } \delta = \frac{1}{2}(s + \sqrt{s^2 + 8s}) \text{ and } s = \frac{-\ln(1 - \beta)}{(m - x^*)f_S}.$$

**PROOF:** First, we solve for  $x^* \leq x$  with  $\beta$ -assurance using Theorem 2. We find  $y^* = z - x^* \geq y$  by applying Lemma 1 to  $Y = \sum_{i=1}^{m-x^*}$ , the sum of  $m - x^*$  independent Bernoulli trials such that  $\Pr[Y_i = 1] = f_S$  trials and  $\mu = (m - x^*)f_S$ :

$$\Pr[Y \geq (1 + \delta)\mu] \leq \text{Exp}\left(-\frac{\delta^2}{2 + \delta}\mu\right),$$

for  $\delta \geq 0$ . We select  $0 < \beta < 1$ , and solve for  $\delta$  using the right hand side of Eq. 9. To bound with high probability, we seek the complement of the right hand side.

$$\beta = 1 - \text{Exp}\left(-\frac{\delta^2}{2 + \delta}(m - x^*)f_S\right) \quad (9)$$

$$\delta = \frac{1}{2}(s + \sqrt{s^2 + 8s}), \text{ where } s = \frac{-\ln(1 - \beta)}{(m - x^*)f_S}. \quad (10)$$

Then, we set

$$y^* = (1 + \delta)(m - x^*)f_S.$$

Since,  $x^* \leq x$  with  $\beta$ -assurance, it follows that  $y^*$  also bounds the sum of  $m - x$  Bernoulli trials, where

$$y^* = (1 + \delta)(m - x)f_S,$$

with probability at least  $\beta$  for any  $\delta \geq 0$  and  $m > 0$ .  $\square$

We validated this theorem empirically as well, as shown in Fig. 20.

## B THEOREM FROM SECTION 5.1

**THEOREM 4:** Relaying a block with  $n$  transactions to a receiver with a mempool (a superset of the block) of  $m$  transactions is more efficient with Graphene Protocol 1 than using an optimally small Bloom filter alone, when the IBLT uses  $k \geq 3$  hash functions. The efficiency gains of Graphene Protocol 1 are  $\Omega(n \log_2 n)$ .

**PROOF:** We assume that  $m = cn$  for some constant  $c > 1$ . Our proof is asymptotic. Thus, according to the law of large numbers, every value  $\delta > 0$  (where  $\delta$  is defined as in Theorem 1) is sufficient to achieve  $\beta$ -assurance when choosing values for  $a^*$ ,  $x^*$ , and  $y^*$ . Accordingly, we may proceed under the assumption that  $\delta = 0$ ; i.e., there is no need to lower the false positive rate of either Bloom filter to account for deviations because the observed false positive rate will always match its expected value asymptotically.

Let  $f$ , where  $0 < f < 1$ , be the FPR of a Bloom filter created in order to correctly identify  $n \geq 1$  elements from a set of  $m \geq 1$  elements. The size of the Bloom filter that has FPR  $f$ , with  $n$  items inserted, is  $-n \log_2(f)$  bits [14]. Let  $f = \frac{p}{m-n}$ , where  $0 < p < 1$ . The expected number of false positives that can pass through the Bloom filter is  $(m - n)\frac{p}{(m-n)} = p$ . Since  $0 < p < 1$ , one out of every  $1/p$  Bloom filters is expected to fail.

To correctly identify the same set of items, Graphene instead uses a Bloom filter with  $f = \frac{a}{m-n}$ , where we set  $a = n/(r\tau)$  since the Bloom filter is optimal, and uses an IBLT with  $a\tau$  cells ( $r$  bytes each) that decodes with probability  $p$ . The expected number of false positives that pass through Graphene's Bloom filter is  $(m - n)\frac{a}{(m-n)} = a$ . An IBLT with 1 to  $a$  items inserted in it decodes with probability  $1 - p$ . In other words, one out of every  $1/p$  Graphene blocks is expected to fail.

The difference in size is

$$\begin{aligned} & -n \log_2\left(\frac{p}{m-n}\right) - \left(-n \log_2\left(\frac{a}{m-n}\right) + a\tau\right) \\ &= n \log_2(a/p) - a\tau \\ &= n(\log_2 n + \log_2^{1/p\tau}) - 1 \\ &= n(\log_2 n + \Omega(\tau^{2-k})) \\ &= \Omega(n \log_2 n), \end{aligned} \quad (11)$$

where Eq. 11 follows from Theorem 1 from Goodrich and Mitzenmacher [30], given that we have an IBLT with  $k \geq 3$  hash functions.  $\square$